

Supporting Information

Repurposing A Long-Wavelength Fluorescent Boronate Probe for the Detection of Reactive Oxygen Species (ROS) in Bacteria

Kai-Cheng Yan,^{a,d} Naing Thet,^a Rachel A. Heylen,^a Adam C. Sedgwick^{*b}, Tony D. James^{*a,c}, A. Toby A. Jenkins^{*a} and Xiao-Peng He^{*d,e}

^aDepartment of Chemistry, University of Bath, Bath, BA2 7AY, U.K.

^bChemistry Research Laboratory, University of Oxford, Mansfield Road, OX1 3TA, U.K.

^cSchool of Chemistry and Chemical Engineering, Henan Normal University, Xinxiang 453007, China.

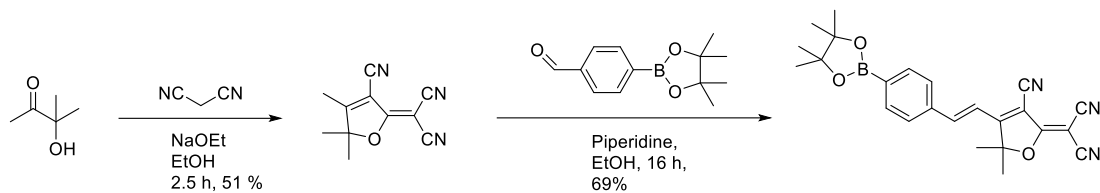
^dKey Laboratory for Advanced Materials and Joint International Research Laboratory of Precision Chemistry and Molecular Engineering, Feringa Nobel Prize Scientist Joint Research Center, School of Chemistry and Molecular Engineering, East China University of Science and Technology, 130 Meilong Rd., Shanghai 200237, China.

^eThe International Cooperation Laboratory on Signal Transduction, Eastern Hepatobiliary Surgery Hospital, National Center for Liver Cancer, Shanghai 200438, China

Table of Contents

1. Experimental	S3
2. Additional Figures and Tables	S6
3. Spectra	S33
4. References	S34

S1. Experimental



Scheme S1. Synthesis of TCF-Bpin.

2-(3-cyano-4,5,5-trimethylfuran-2(5H)-ylidene)malononitrile (TCF) and **(E)-2-(3-cyano-5,5-dimethyl-4-(4-(4,4,5,5-tetramethyl-1,3,2-dioxaborolan-2-yl)styryl)furan-2(5H)-ylidene)malononitrile (TCF-Bpin)** These compounds were synthesized with guidance by literature methods.¹

The auxiliary chemicals used in the study are commercially available. Thin-layer chromatography (TLC) was performed on silica gel plates and visualized by UV to track the reaction. Nuclear Magnetic Resonance (NMR) characterizations were recorded by an Agilent ProPulse 500 spectrometer. Fluorescence emission measurements were performed on a BMG Labtech CLARIO star plate reader using Greiner Bio-One microplates (96-well, black-walled). Data were collected via the BMG Labtech Clariostar data analysis software package MARS. UV-Vis absorption measurements were performed on a Varian Cary 500 UV-Vis spectrophotometer. Fluorescence imaging was carried out on a ZEISS LSM-880 Inverted Confocal Laser Scanning Microscope equipped with 561 nm laser source, where samples were prepared on microscopy glass slides. The fluorescence intensities of the images were calculated by Image-J. The pH values were measured on a Hanna Instruments HI 9321 Microprocessor pH meter which was routinely calibrated using Fisher Chemicals standard buffer solutions.

The strains used include *P. aeruginosa* PAO1 and *S. aureus* NCTC 10788. Single colonies were transferred to Mueller Hinton broth and then incubated with shaking at 37 °C overnight, followed by the subculture in fresh Mueller Hinton broth for the following use.

Table S1. List of bacterial isolates.

Strains	Information	Ref
PAO1	Reference strain, a mutant of the original PAO strain isolated in 1954 from a wound in Melbourne, Australia.	2,3
NCTC 10788	PHE reference strain. Methicillin sensitive.	4,5

The Minimum Inhibitory Concentrations were determined according to the Clinical and Laboratory Standards Institute (CLSI) guidelines. Briefly, aqueous antibiotic solutions were added to a 96 well plate and serially diluted two-fold by Mueller Hinton broth. Overnight cultures of bacteria were sub-cultured in fresh Mueller Hinton broth, before adding to all relevant wells in the 96 well plate. Bacteria only and broth only controls were carried out in tandem. After overnight inhibition the plates were read to determine the optical densities at 600 nm.

Planktonic samples were further diluted to 10^1 , 10^2 , 10^3 , 10^4 , and 10^5 times by sterile water. Diluents of each group were all dropped on Mueller Hinton agar plate (or alternatively Brain-Heart Infusion agar plate) for three times, dried, and incubated at 37°C overnight. Then, the numbers of average colony forming units (CFUs) and the standard deviations (between three repetitions) were counted and calculated.

S2. Additional Figures and Tables

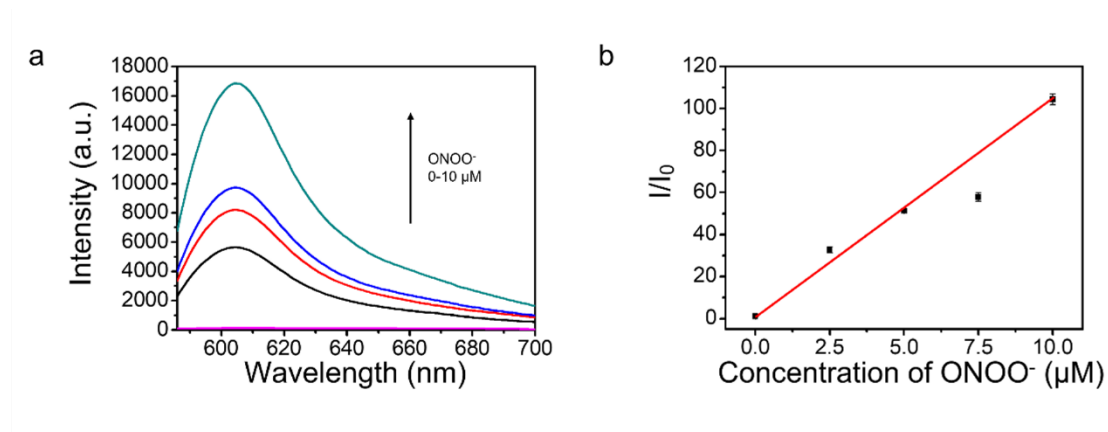


Figure S1. (a) Fluorescence spectra of **TCF-Bpin** (10 μM , dissolved in DMSO) with the addition of ONOO^- (0 - 10 μM) in PBS buffer solution (pH = 7.40). $\lambda_{\text{ex}} = 560$ nm. (b) The relationship between the fluorescence emission change and ONOO^- concentrations. Black: 2.5 μM ; Red: 5 μM ; Blue: 7.5 μM ; Green: 10 μM . $\lambda_{\text{ex}} = 560$ nm, $\lambda_{\text{em}} = 606$ nm.

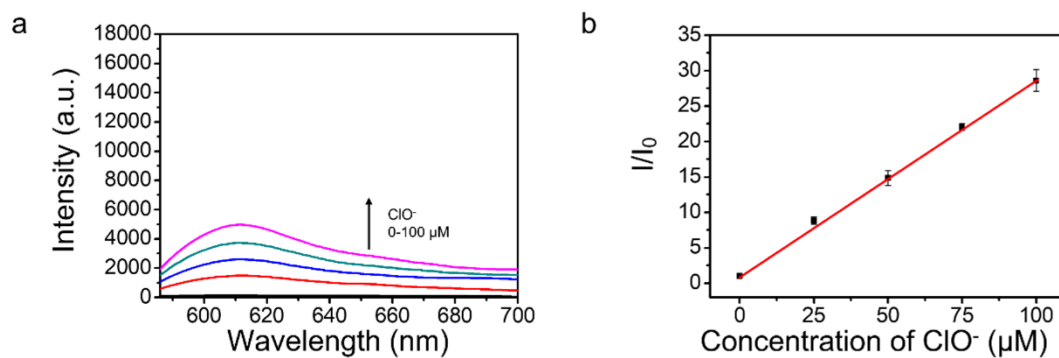


Figure S2. (a) Fluorescence spectra of **TCF-Bpin** (10 μM, dissolved in DMSO) with the addition of ClO⁻ (0 - 100 μM) in PBS buffer solution (pH = 7.40). $\lambda_{\text{ex}} = 560$ nm. (b) The relationship between the fluorescence emission change and ClO⁻ concentrations. Red: 25 μM; Blue: 50 μM; Green: 75 μM; Pink: 100 μM. $\lambda_{\text{ex}} = 560$ nm, $\lambda_{\text{em}} = 606$ nm.

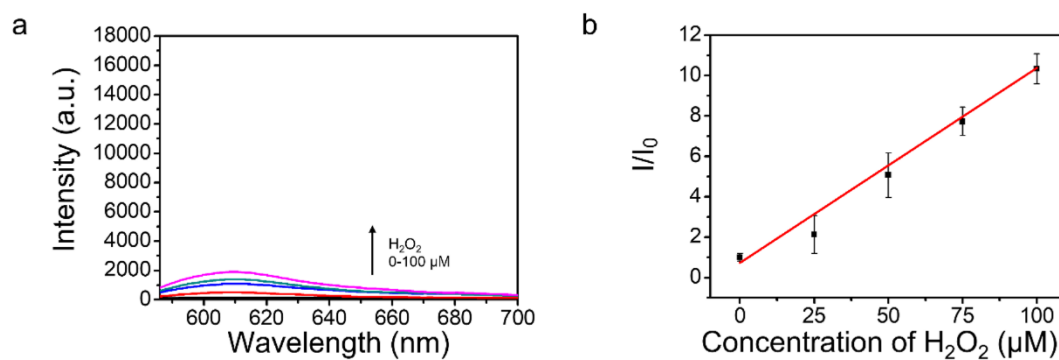


Figure S3. (a) Fluorescence spectra of **TCF-Bpin** (10 μM, dissolved in DMSO) with the addition of H₂O₂ (0 - 100 μM) in PBS buffer solution (pH = 7.40). $\lambda_{\text{ex}} = 560$ nm. (b) The relationship between the fluorescence emission change and H₂O₂ concentrations. Red: 25 μM; Blue: 50 μM; Green: 75 μM; Pink: 100 μM. $\lambda_{\text{ex}} = 560$ nm, $\lambda_{\text{em}} = 606$ nm.

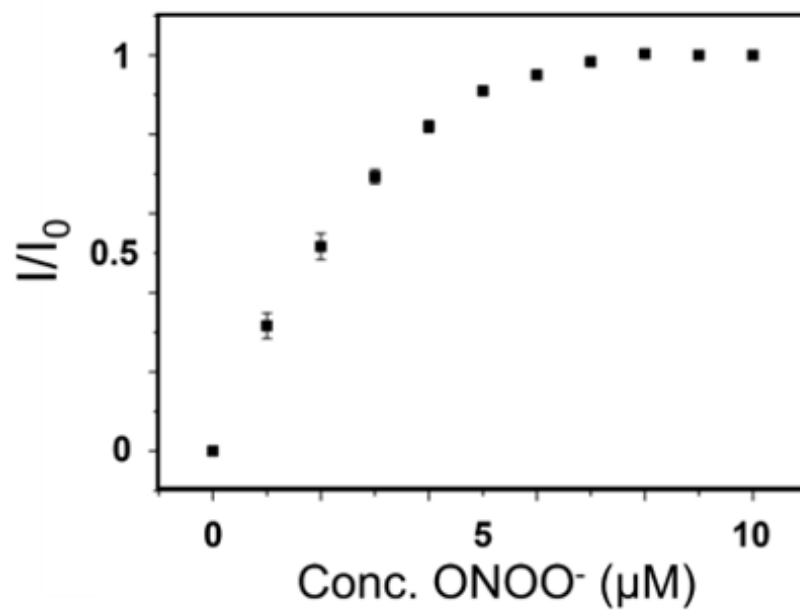


Figure S4. Plotting the relationship between fluorescence emission change and the concentration of ONOO⁻ (0 - 10 μM) at low level to determine the sensitivity of probe **TCF-Bpin**.¹

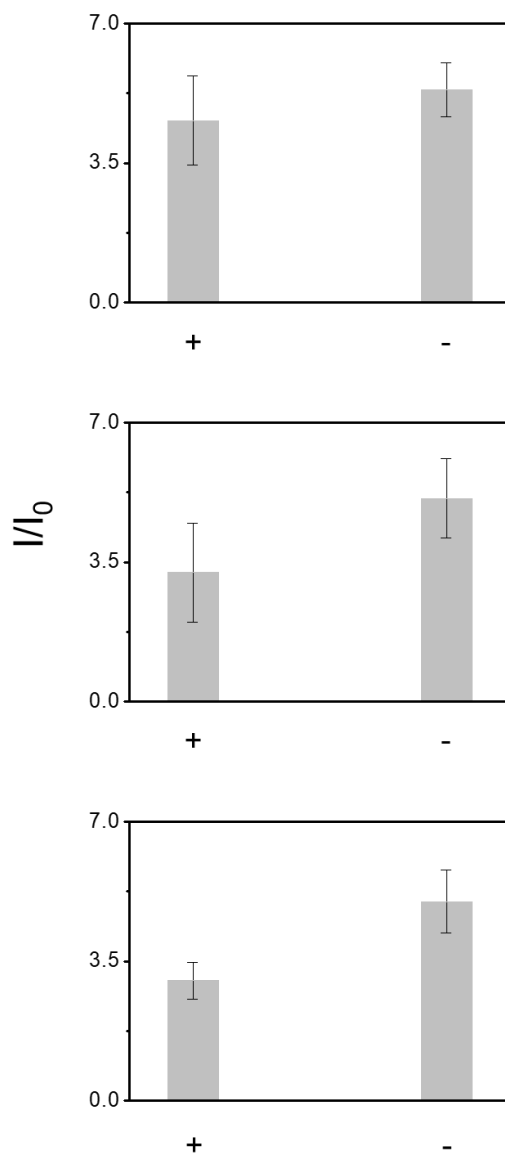


Figure S5. The fluorescence emission change of **TCF-Bpin** (10 μM) upon activation of 10 μM ONOO^- (top), 100 μM ClO^- (middle), or 100 μM H_2O_2 (bottom), with (+) or without (-) presence of GSH (100 μM).



Figure S6. The plate reader detection of OD₆₀₀ absorption intensities of the MIC well plates (a) and the corresponding bar charts (b) in the MIC trial of Chloramphenicol towards *S. aureus* and *P. aeruginosa*, and the selected sub-MIC wells (yellow) for the subsequent detection by probe **TCF-Bpin**.



Figure S7. The plate reader detection of OD₆₀₀ absorption intensities of the MIC well plates (a) and the corresponding bar charts (b) in the MIC trial of Tetracycline towards *S. aureus* and *P. aeruginosa*, and the selected sub-MIC wells (yellow) for the subsequent detection by probe **TCF-Bpin**.



Figure S8. The plate reader detection of OD₆₀₀ absorption intensities of the MIC well plates (a) and the corresponding bar charts (b) in the MIC trial of Ciprofloxacin towards *S. aureus* and *P. aeruginosa*, and the selected sub-MIC wells (yellow) for the subsequent detection by probe **TCF-Bpin**.

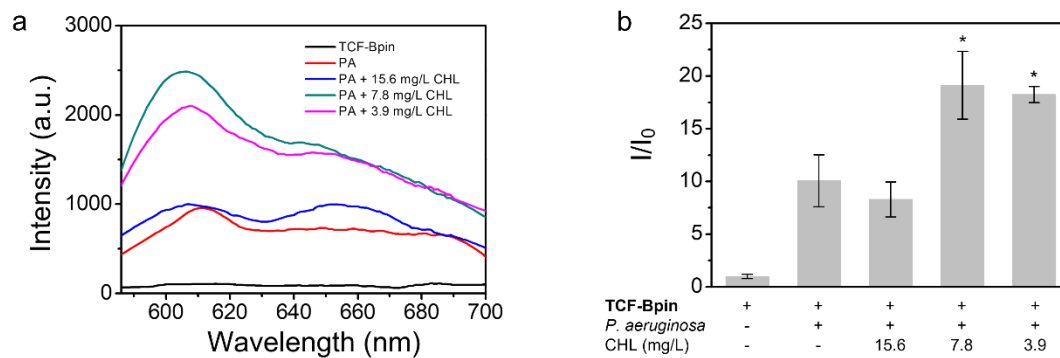


Figure S9. (a) Fluorescence spectra of **TCF-Bpin** with presence of *P. aeruginosa* (PA) without antibiotic treatment (control) and *P. aeruginosa* picked out from the MIC plate wells with treatment of sub-MIC concentrations of Chloramphenicol (CHL). (b) Corresponding change in fluorescence. $\lambda_{\text{ex}} = 560 \text{ nm}$, $\lambda_{\text{em}} = 606 \text{ nm}$.

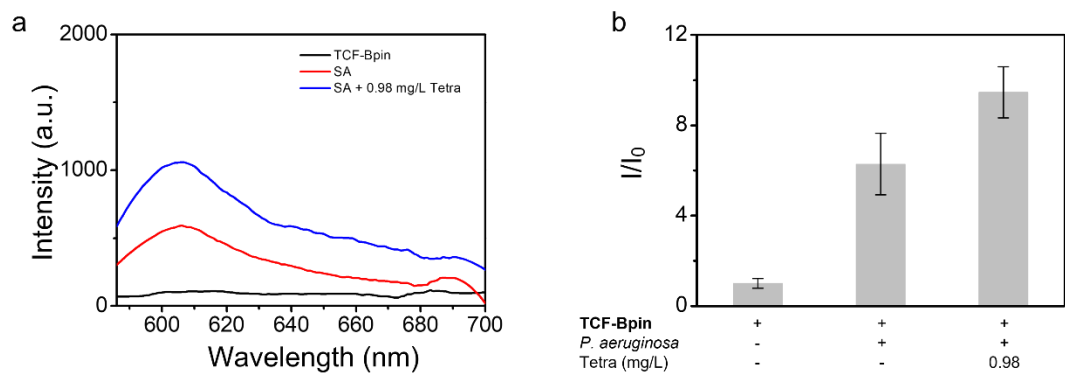


Figure S10. (a) Fluorescence spectra of **TCF-Bpin** with presence of *S. aureus* (SA) without antibiotic treatment (control) and *S. aureus* picked out from the MIC plate wells with treatment of sub-MIC concentrations of Tetracycline (Tetra). (b) Corresponding change in fluorescence. $\lambda_{ex} = 560$ nm, $\lambda_{em} = 606$ nm.

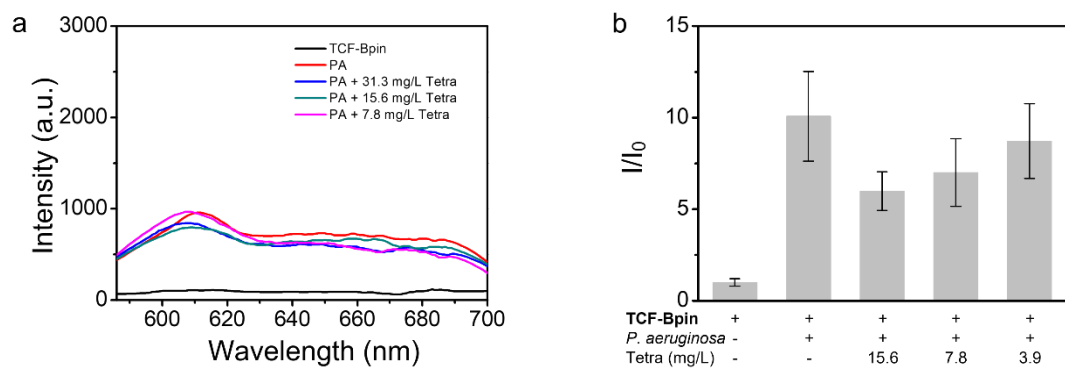


Figure S11. (a) Fluorescence spectra of **TCF-Bpin** with presence of *P. aeruginosa* (PA) without antibiotic treatment (control) and *P. aeruginosa* picked out from the MIC plate wells with treatment of sub-MIC concentrations of Tetracycline (Tetra). (b) Corresponding change in fluorescence. $\lambda_{ex} = 560$ nm, $\lambda_{em} = 606$ nm.

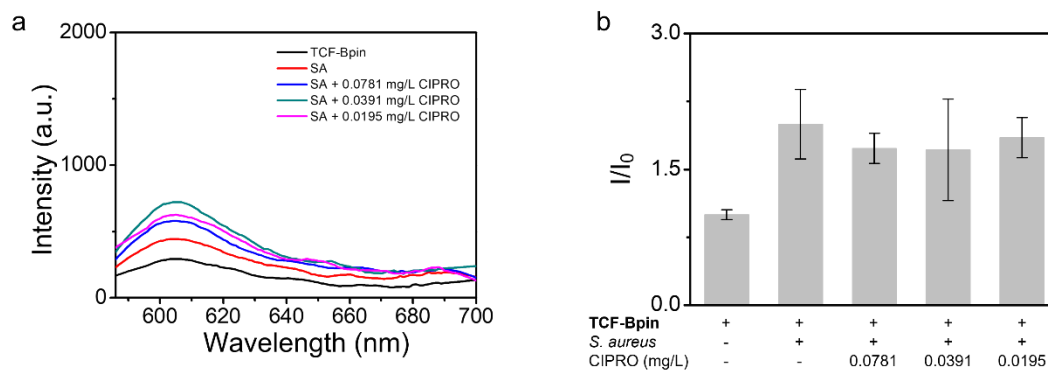


Figure S12. (a) Fluorescence spectra of **TCF-Bpin** with presence of *S. aureus* (SA) without antibiotic treatment (control) and *S. aureus* picked out from the MIC plate wells with treatment of sub-MIC concentrations of Ciprofloxacin (Cipro). (b) Corresponding change in fluorescence. $\lambda_{ex} = 560$ nm, $\lambda_{em} = 606$ nm.

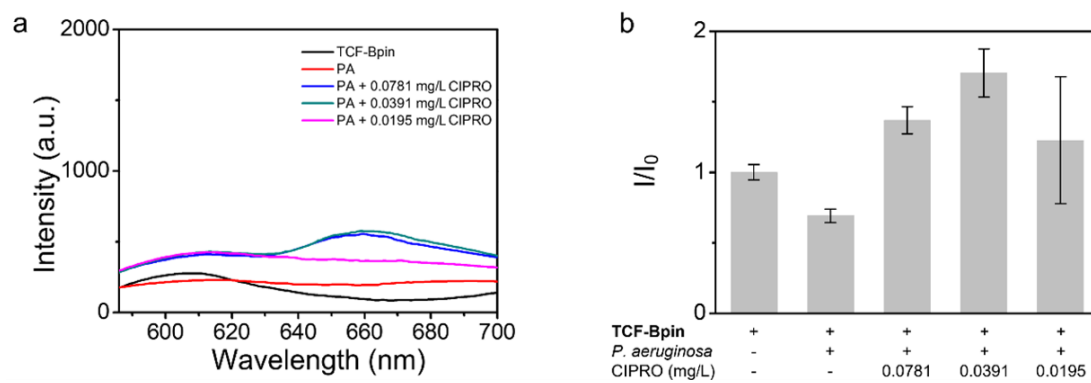


Figure S13. (a) Fluorescence spectra of **TCF-Bpin** with presence of *P. aeruginosa* (PA) without antibiotic treatment (control) and *P. aeruginosa* picked out from the MIC plate wells with treatment of sub-MIC concentrations of Ciprofloxacin (Cipro). (b) Corresponding change in fluorescence. $\lambda_{\text{ex}} = 560 \text{ nm}$, $\lambda_{\text{em}} = 606 \text{ nm}$.

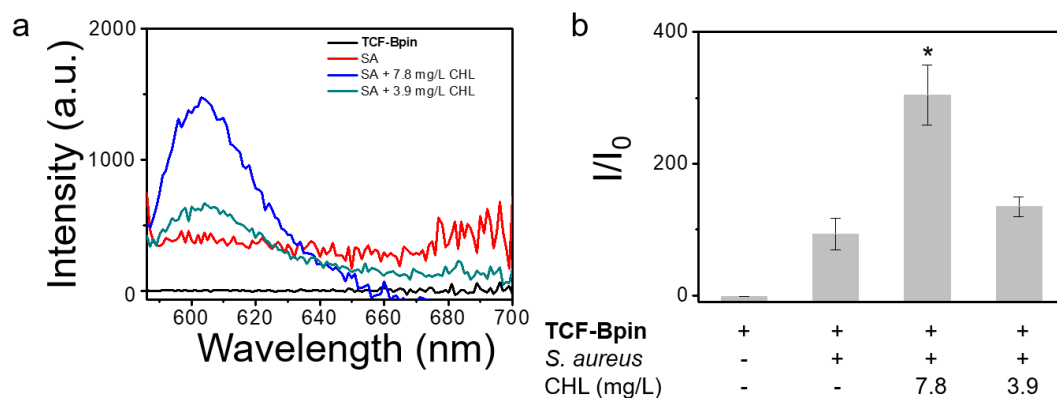


Figure S14. (a) Fluorescence spectra of **TCF-Bpin** with presence of multidrug-resistant *S. aureus* (SA) without antibiotic treatment (control) and *S. aureus* with treatment of different sub-MIC concentrations of Chloramphenicol (CHL). (b) Corresponding change in fluorescence. $\lambda_{\text{ex}} = 560 \text{ nm}$, $\lambda_{\text{em}} = 606 \text{ nm}$.

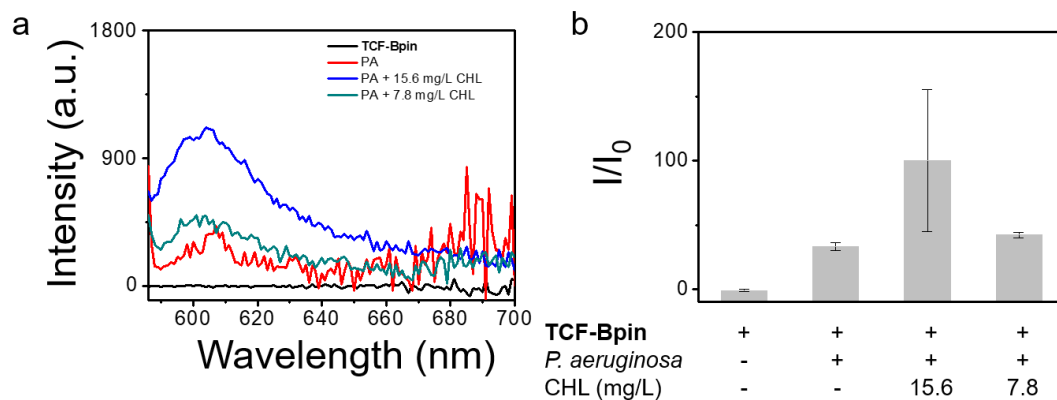


Figure S15. (a) Fluorescence spectra of **TCF-Bpin** with presence of multidrug-resistant *P. aeruginosa* (PA) without antibiotic treatment (control) and *P. aeruginosa* with treatment of different sub-MIC concentrations of Chloramphenicol (CHL). (b) Corresponding change in fluorescence. $\lambda_{\text{ex}} = 560 \text{ nm}$, $\lambda_{\text{em}} = 606 \text{ nm}$.

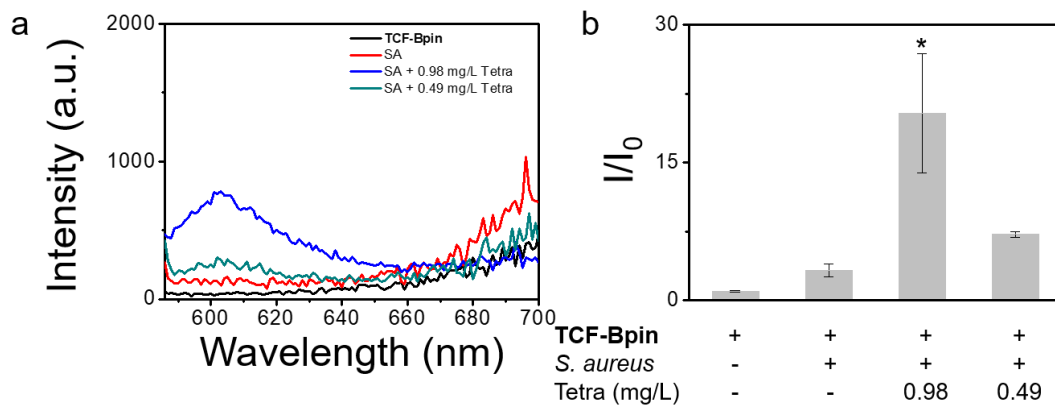


Figure S16. (a) Fluorescence spectra of **TCF-Bpin** with presence of multidrug-resistant *S. aureus* (SA) without antibiotic treatment (control) and *S. aureus* with treatment of different sub-MIC concentrations of Tetracycline (Tetra). (b) Corresponding change in fluorescence.

$\lambda_{\text{ex}} = 560 \text{ nm}$, $\lambda_{\text{em}} = 606 \text{ nm}$.

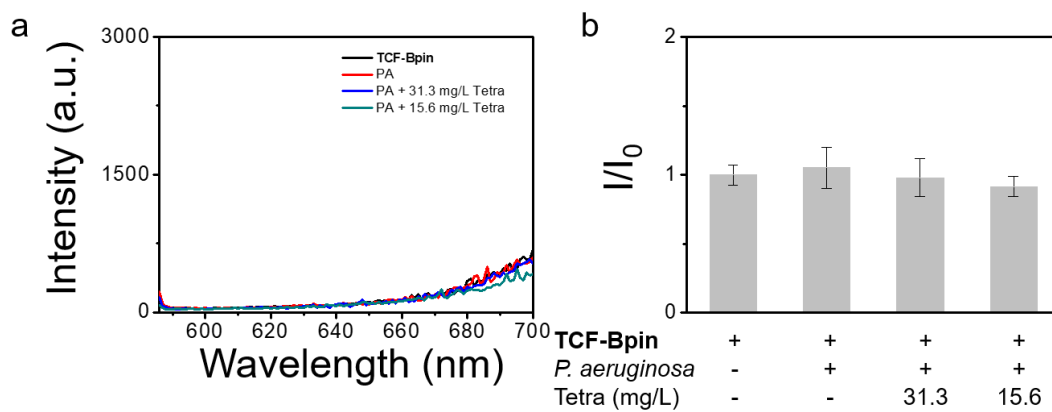


Figure S17. (a) Fluorescence spectra of **TCF-Bpin** with presence of multidrug-resistant *P. aeruginosa* (PA) without antibiotic treatment (control) and *P. aeruginosa* with treatment of different sub-MIC concentrations of Tetracycline (Tetra). (b) Corresponding change in fluorescence. $\lambda_{\text{ex}} = 560 \text{ nm}$, $\lambda_{\text{em}} = 606 \text{ nm}$.

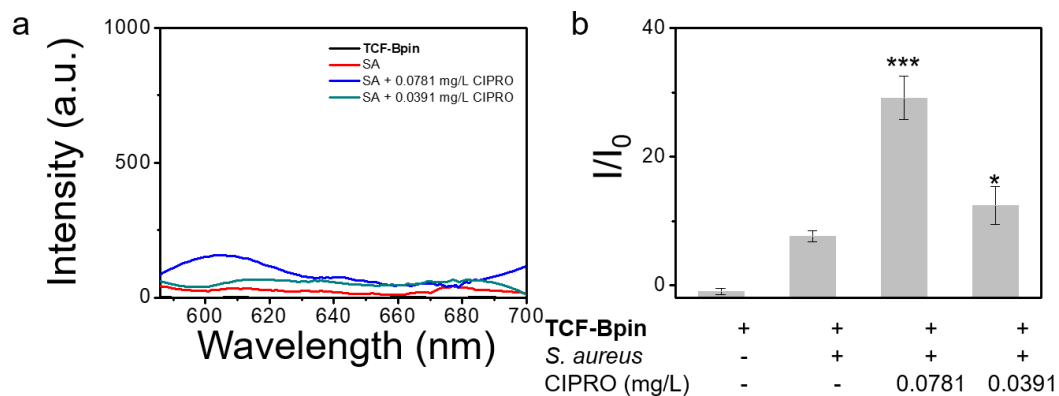


Figure S18. (a) Fluorescence spectra of **TCF-Bpin** with presence of multidrug-resistant *S. aureus* (SA) without antibiotic treatment (control) and *S. aureus* with treatment of different sub-MIC concentrations of Ciprofloxacin (Cipro). (b) Corresponding change in fluorescence. $\lambda_{\text{ex}} = 560 \text{ nm}$, $\lambda_{\text{em}} = 606 \text{ nm}$.

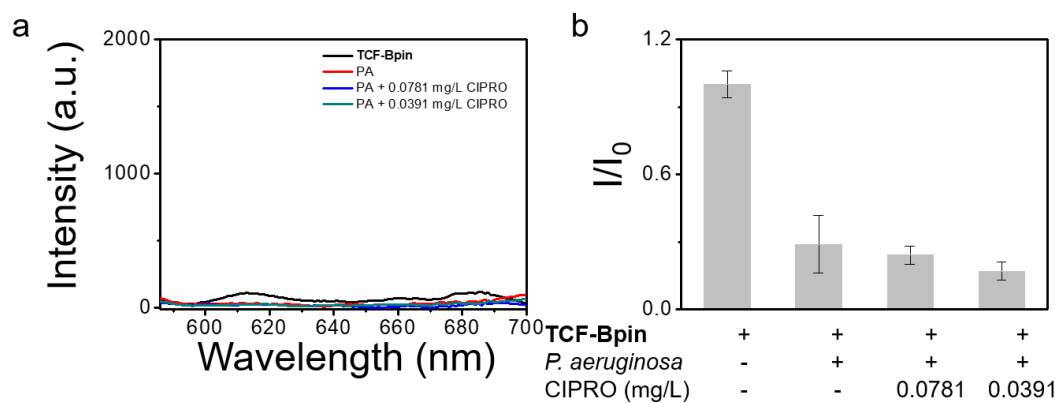


Figure S19. (a) Fluorescence spectra of **TCF-Bpin** with presence of multidrug-resistant *P. aeruginosa* (PA) without antibiotic treatment (control) and *P. aeruginosa* with treatment of different sub-MIC concentrations of Ciprofloxacin (Cipro). (b) Corresponding change in fluorescence. $\lambda_{\text{ex}} = 560 \text{ nm}$, $\lambda_{\text{em}} = 606 \text{ nm}$.

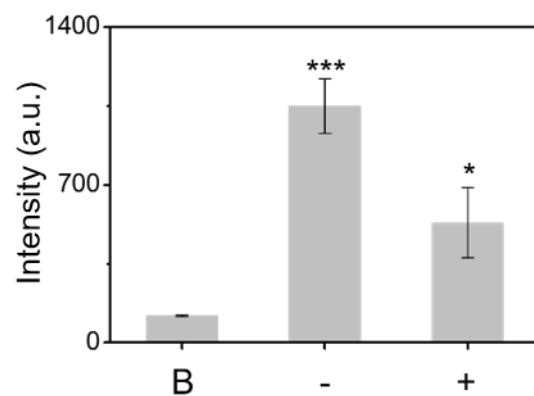


Figure S20. Fluorescence emission changes of Chloramphenicol-treated sub-MIC *S.*

aureus without (-) or with (+) presence of ONOO⁻ inhibitor. $\lambda_{\text{ex}} = 560 \text{ nm}$, $\lambda_{\text{em}} = 606 \text{ nm}$.

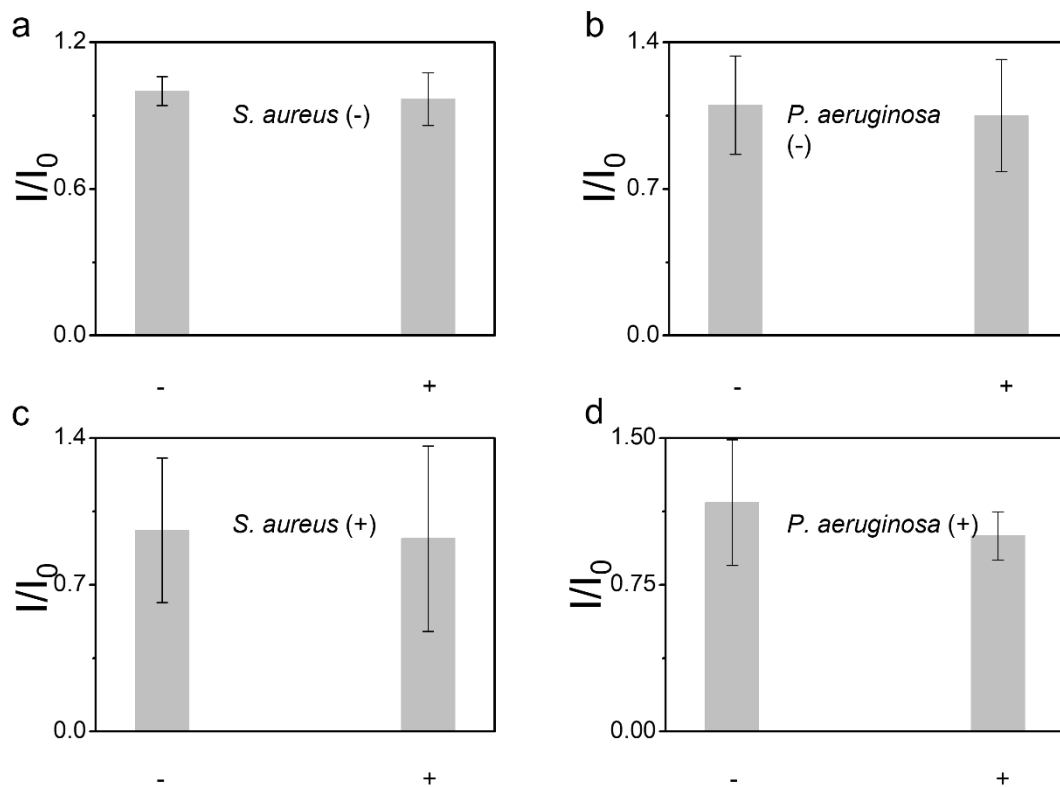


Figure S21. Fluorescence emission changes of TCF-Bpin incubated with non-stressed common (-) or drug-resistant (+) bacteria, compared with probe only. $\lambda_{\text{ex}} = 560 \text{ nm}$, $\lambda_{\text{em}} = 606 \text{ nm}$.

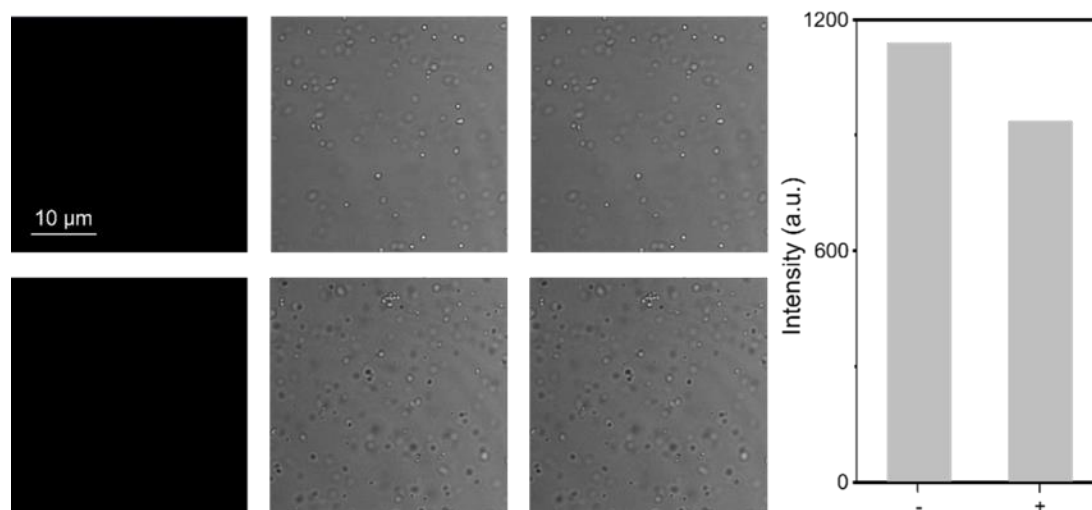


Figure S22. Confocal Laser-Scanning Microscope images and intensity change of **TCF-Bpin** incubated Tetracycline-treated *S. aureus* without (above) or with (below) presence of ONOO⁻ inhibitor. $\lambda_{\text{ex}} = 561$ nm laser source), $\lambda_{\text{em}} = 606$ nm.

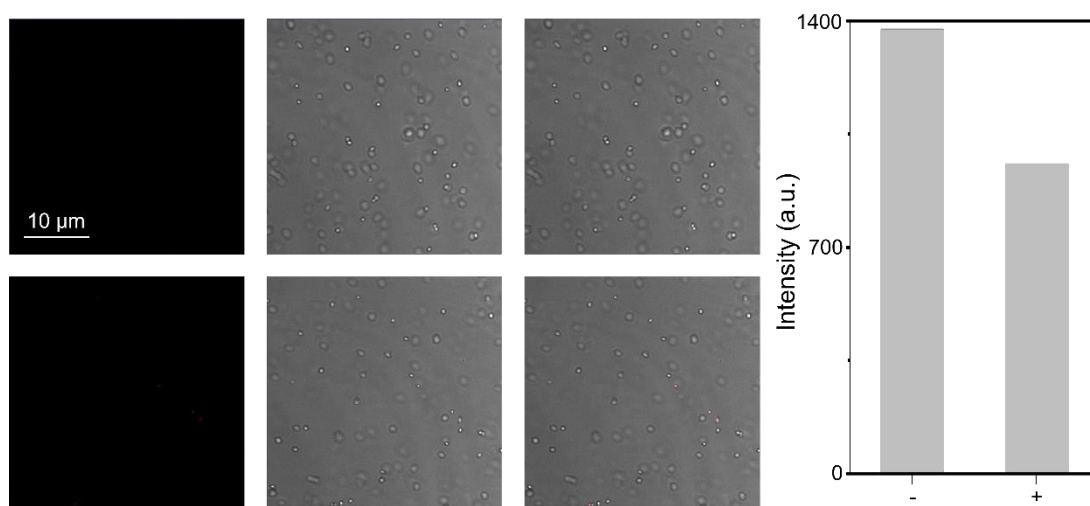


Figure S23. Confocal Laser-Scanning Microscope images and intensity change of **TCF-Bpin** incubated Ciprofloxacin-treated *S. aureus* without (above) or with (below) presence of ONOO⁻ inhibitor. $\lambda_{\text{ex}} = 561$ nm laser source), $\lambda_{\text{em}} = 606$ nm.

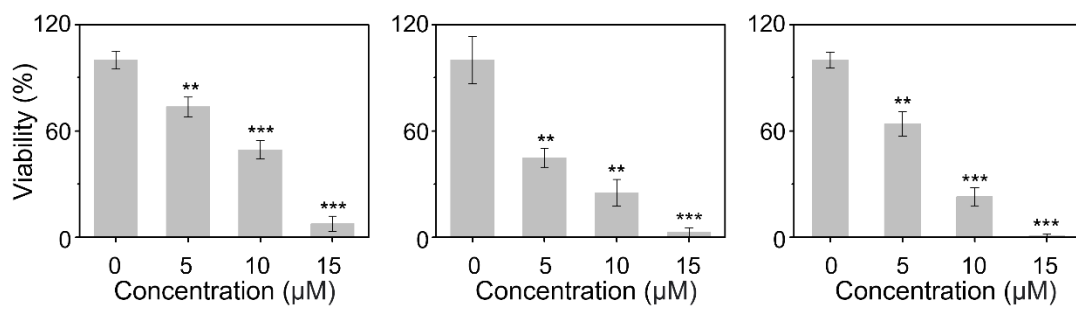


Figure S24. Percentage *S. aureus* viability after treatment of ONOO⁻ (left), H₂O₂ (middle), and ClO⁻ (right).

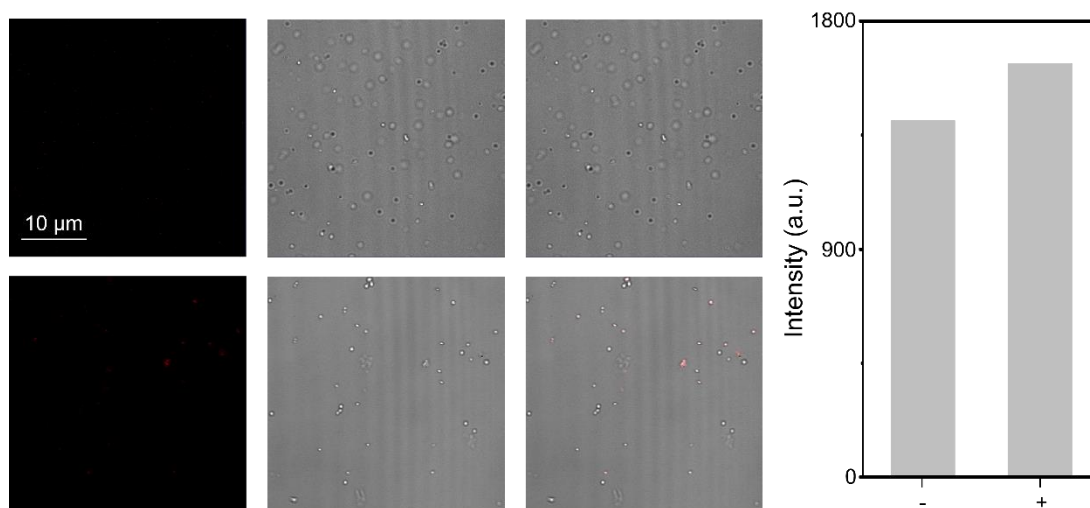


Figure S25. Confocal Laser-Scanning Microscope images and intensity change of **TCF-Bpin** incubated *S. aureus* without (above) or with (below) incubation of ClO^- ($10 \mu\text{M}$). $\lambda_{\text{ex}} = 561 \text{ nm}$ laser source, $\lambda_{\text{em}} = 606 \text{ nm}$.

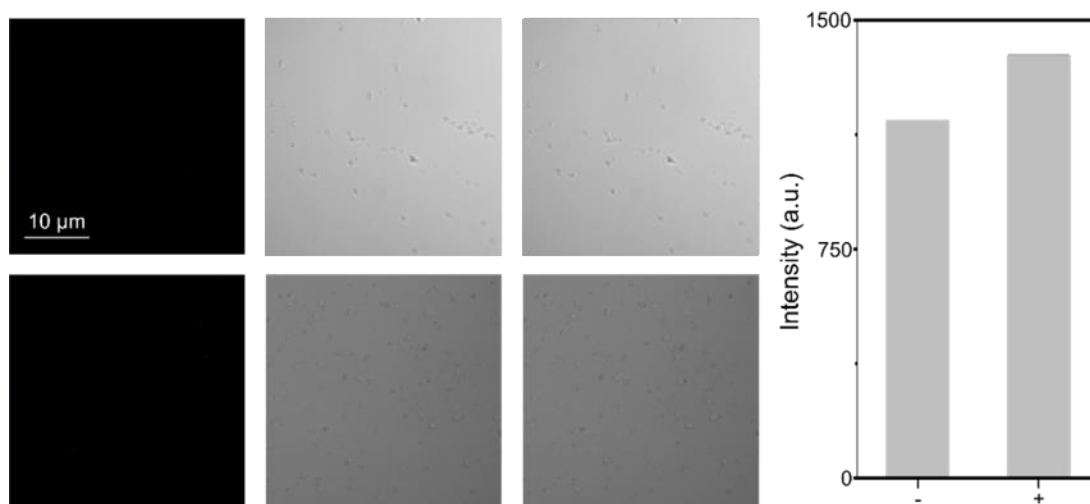


Figure S26. Confocal Laser-Scanning Microscope images and intensity change of **TCF-Bpin** incubated *S. aureus* without (above) or with (below) incubation of H₂O₂ (10 μM). λ_{ex} = 561 nm laser source, λ_{em} = 606 nm.

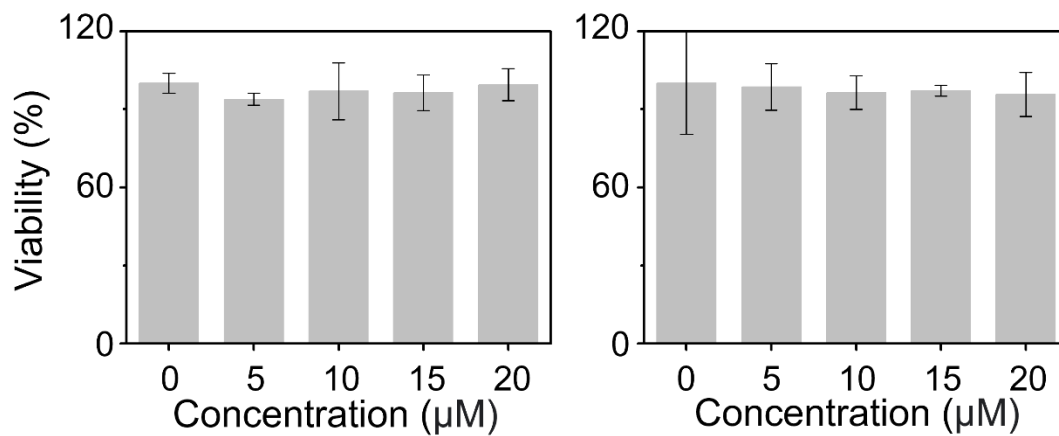
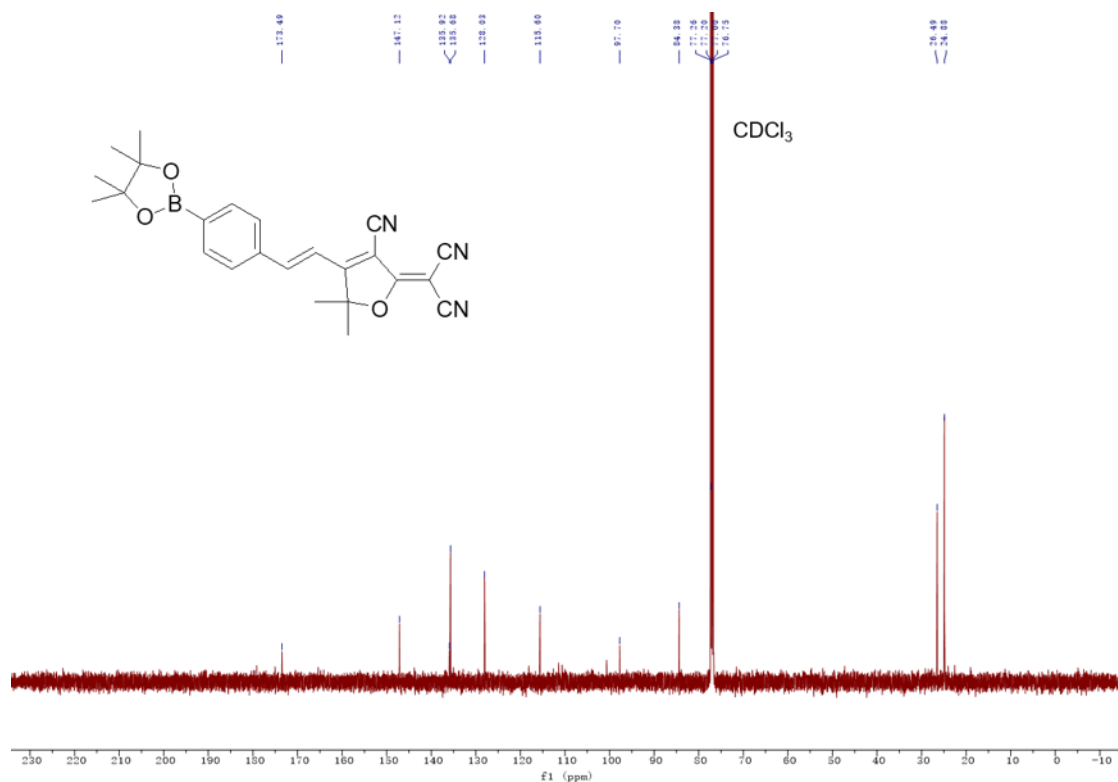
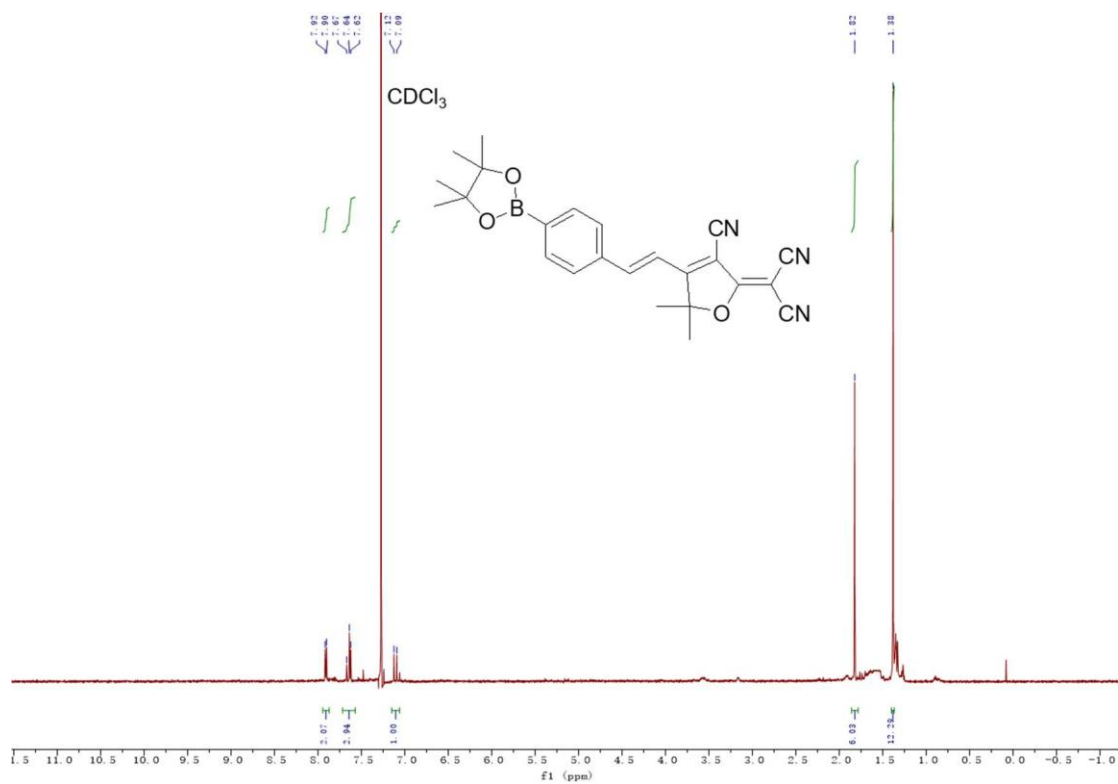


Figure S27. Percentage *S. aureus* (left) and *P. aeruginosa* (right) viability after treatment of TCF-Bpin.

S3. Spectra



S4. References

1. A. C. Sedgwick, H.-H. Han, J. E. Gardiner, S. D. Bull, X.-P. He, T. D. James. *Chem. Commun.*, **2017**, 53, 12822.
2. J. Klockgether, A. Munder, J. Neugebauer, C. F. Davenport, F. Stanke, K. D. Larbig, S. Heeb, U. Schock, T. M. Pohl, L. Wiehlmann, B. Tumbler. *J. Bacteriol.*, **2010**, 192, 1113.
3. B. W. Holloway. *Microbiology*, **1955**, 13, 572.
4. <https://www.pheculturecollections.org.uk/products/bacteria/detail.jsp?refId=NCTC%2010788&collection=nctc>.
5. C. Shaw, J. M. Stitt, S. T. Cowan. *Microbiology*, **1951**, 5, 1010.